Contents lists available at ScienceDirect

Arabian Journal of Chemistry

journal homepage: www.sciencedirect.com

Original article

Mild and economy homogeneous UV-LED/persulfate process for degradation of fluoxetine model drug

Javad Saien *, Hadi Karbalaei Abbas, Farnaz Jafari

Faculty of Chemistry and Petroleum Science, Bu-Ali Sina University, Hamedan, Iran

ABSTRACT

A homogeneous persulfate (PS) activation under low energy consumption ultraviolet light-emitting diodes (UV-LEDs) was established in order to degrade the resistive fluoxetine-hydrochloride drug in aqueous media. For this aim, a falling film photo-reactor, equipped with four arrays of six UV-LEDs (395 nm, 1 W each), was utilized. Trace concentrations of ferrous sulfate and heating the media could significantly improve the degradation efficiency. Under the established optimal conditions of 100 mg/L of persulfate, 1 mg/L of ferrous sulfate, natural pH of 6.4 and temperature of 40 °C, a 71.1% degradation efficiency was achieved for 40 mg/L fluoxetine initial concentration after 50 min. The kinetic study revealed a pseudo-first order overall degradation rate. Based on scavenger quenching results, it was revealed that the hydroxyl radical and sulfate anion radical had, respectively, 52.3 and 31.4% contribution in degradation. To extend results to real conditions, the influence of inorganic cations/anions and also humic acid was investigated. From LC-MS analysis results, the transformation products were identified and three degradation pathways were proposed. Interestingly, a cost evaluation indicated electrical energy consumption of 16.7 kWh/m^3 and operating cost of only $1.71 per each cubic meter. Consistently, the profound UV-LED/PS/Fe^{2+}/heat process exhibited desired capabilities in scenarios for treating resistive drug wastewaters.

© 2023 The Author(s). Published by Elsevier B.V. on behalf of King Saud University. This is an open access article under the CC BY-NC-ND license (http://creativecommons.org/licenses/by-nc-nd/4.0/).

1. Introduction

There is an increasing demand for pharmaceuticals to save billions of lives; but they are also considered as emerging pollutants in wastewaters. The evidences of water contamination by pharmaceuticals have taken them to the list of wastewater emerging pollutants because of expansion in drug usage. Pharmaceuticals can create significant adverse environmental and human health impacts even at low concentrations (Rasheed et al. 2021; Taoufik et al. 2021). Antibiotics, chemotherapy products, analgesics, antipyretics, and being in its majority, antidepressants as the prevalence of psychiatric disorders (Sicras-Mainar and Navarro-Artieda, 2016) are among the main pharmaceutical pollutants (Tiwari et al., 2017).

Fluoxetine-hydrochloride (FLX-HCl, simply FLX) is an antidepressant and a selective serotonin reuptake inhibitor. Some studies indicate that FLX cannot be removed in aqueous media by hydrolysis or photolysis, having persistence for more than 100 days and not being affected by biodegradation in long times more than 60 days (Kwon and Armbrust, 2009; Redshaw et al., 2008; Méndez-Arriag et al., 2011). This drug has been detected in the aquatic environment worldwide with surface water ranging from 0.066 to 0.929 µg/L (Martin et al. 2017).

Advanced oxidation processes (AOPs) are effective techniques currently used for the degradation of different pollutants. The basis is the production of active radicals such as hydroxyl and sulfate anion radicals. Mineralization of organic pollutants into ultimate non-toxic inorganic compounds, and providing no secondary polluted media are the advantages of AOPs (Kanakaraju et al., 2018; Saien and Bazkiaei, 2018). Accordingly, homogeneous photochemical processes based on ultraviolet/photo-persulfate have attracted much attention. One major advantage is neglecting solid catalysts and thus, no need to recovery (Hoang et al., 2022; Saien and Seyyedan, 2019; Duan et al., 2017). Peroxydisulfate, simply persulfate (PS) is a powerful oxidant, capable of degrading recalcitrant pollutants in homogeneous processes. Different PS salts of potas-

* Corresponding author.
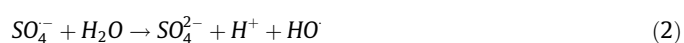E-mail address: saien@basu.ac.ir (J. Saien).
Peer review under responsibility of King Saud University.

Production and hosting by Elsevier

sium, ammonium and sodium can be utilized, commercially available and stable in their solid state.

Persulfate can be activated with and without external energy aided methods. Those dealing with external energy include heat, microwave, ultrasonic, photo and electrochemical activation methods; and those with no external energy activation include alkaline, organic substrate and catalytic activation. Details of persulfate activation, for the aim of pollutants degradation, have been reported in a recent publication (Saien and Jafari, 2022).

Upon activation in aqueous media, PS generates sulfate anion radical (SO_4^-) and hydroxyl radical ($HO^.$) with high redox potentials (2.5–3.1 V for SO_4^- and 1.8–2.7 V for $HO^.$). Compared to hydroxyl radical, sulfate anion radical exhibits nonselective impact and longer lifetime (Cai et al., 2021). Among the various persulfate activation methods, photo irradiation stands out as a low-cost and environmentally friendly method (Pourehie and Saien, 2020). By irradiating, the peroxide bonds break by electromagnetic waves to form two sulfate anion radicals. The reaction mechanism can be explained briefly by the following reactions (Lau et al., 2007):

$$S_2O_8^{2-} \xrightarrow{h\nu} 2SO_4^- \tag{1}$$

$$SO_4^- + H_2O \rightarrow SO_4^{2-} + H^+ + HO^. \tag{2}$$

$$SO_4^- + OH^- \rightarrow SO_4^{2-} + HO^. \tag{3}$$

$$S_2O_8^{2-} + HO^. \rightarrow S_2O_8^- + OH^- \tag{4}$$

$$SO_4^{2-} + HO^. \rightarrow SO_4^- + OH^- \tag{5}$$

Indeed, light emission source and the irradiation wavelength are essential to initiate and drive these reactions. For this aim, ultraviolet lights are mostly utilized, categorized in three classes of UV-A (wavelength within 315–400 nm), UV-B (within 280–315 nm) and UV-C (within 100–280 nm). However, in UV technology, mercury lamps are with numerous risks (Matafonova and Batoev, 2018). As of now, the new generation of light sources, ultraviolet light-emitting diodes (UV-LEDs) are classified into near-UV (NUV) and deep-UV (DUV) LEDs, emitting at 300 – 400 nm and 200–300 nm, respectively (Muramoto et al., 2014). The utilization of UV-LEDs as the light source provides high efficiency due to its unique features of safe irradiation in the absence of mercury (Chen et al., 2017), low energy consumption, long lifetime and easier temperature control because of low heat generation. Further, the outstanding merit of UV-LEDs is attributed to the design adoptability with small size for each LED (Marchetti and Azevedo, 2020). These benefits have led to focusing more on the use of UV-LEDs in wastewater treatments instead of conventional lamps (Eskandarian et al., 2021, Cai et al., 2021).

Transition metal ions like Fe^{2+}, Ag^+, Mn^{2+}, Cu^{2+} and Co^{2+}, on the other hand, have been authenticated to effectively activate persulfate. The most commonly used transition metal, ferrous ion, Fe^{2+}, gives rise the activation via generating ferric ions and then regeneration (Chakma et al., 2017) as:

$$Fe^{2+} + S_2O_8^{2-} \rightarrow Fe^{3+} + SO_4^- + SO_4^{2-} \tag{6}$$

$$Fe^{3+} + S_2O_8^{2-} \rightarrow Fe^{2+} + 2SO_4^- \tag{7}$$
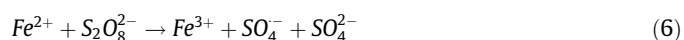
Previous studies on employing such process includes degradation of acetaminophen employing different UV-LED/chloramine, UV-LED/hydrogen peroxide, and UV-LED/persulfate (Li et al. 2020). In a study by Cai et al. (2021), the oxidation of carbamazepine by UV-LED/PS and UV-LED/H_2O_2 processes was investigated with trace amount of copper ion. Recently, the ability of UV-LED/PS process with trace amount of 2,2,6,6-tetramethylpiperidine-N-oxyl was investigated for degradation of chloroquine phosphate as an antiviral drug used for the treatment of corona virus disease (Sun et al., 2022).

These advancements encouraged the authors to employ this method for degradation of fluoxetine-HCl drug by means of a falling film photoreactor. For this aim, trace amounts of ferrous sulfate can favor sulfate anion radical generation. The fluoxetine-HCl drug has been designed with high chemical stability to reach and interact with target molecules in human body (Silva et al., 2012). In the employed process, the influence of different parameters is investigated and optimum conditions are sought. The contribution of active radicals is determined by scavenger quenching experiments. The influence of water matrix cations/anions as well as humic acid are considered. In addition, transformation products, the degradation kinetic and the level of energy consumption are investigated. Development of such novel strategies seems quite useful for degradation of pharmaceutical compounds in water.

2. Experimental

2.1. Materials and reagents

Fluoxetine hydrochloride ($C_{17}H_{19}ClF_3NO$, MW 345.8) was purchased from Pars Darou company, 99.1% pure. Ferrous sulfate heptahydrate ($FeSO_4.7H_2O$, 99.5%), potassium persulfate ($K_2S_2O_8$, 99%), sodium hydroxide ($NaOH$, 97%), hydrochloric acid (HCl, 37%), tert-butyl alcohol ($C_4H_{10}O$, 99%), ethanol (C_2H_5OH, 99%), tetrahydrofuran (THF) (C_4H_8O, 99.8%), 1,4-benzoquinone (BQ) ($C_6H_4O_2$, 99.8%), sodium salt humic acid ($C_9H_8Na_2O_4$, 99.1%), sodium chloride ($NaCl$, 99.5%), calcium chloride ($CaCl_2$, 99.8%), sodium bicarbonate ($NaHCO_3$, 99.5%) and calcium phosphate ($Ca_3(PO_4)_2$, 99.8%) were Merck products. Dilute solutions of sodium hydroxide and hydrochloric acid were used for adjusting the pH of solutions. In addition, tert-butyl alcohol (Merck, 99%) and ethanol (Merck, 99.5%) were used for scavenging radicals. Deionized water (conductivity less than 0.08 μS/cm) was utilized in preparing solutions and precise investigating the effects of each parameter.

2.2. The photo-reactor and procedure

The used photo-reactor set-up, was a cubic rectangular stainless steel space with the capacity of about one liter (Fig. 1). 24 UV-LEDs (Epileds, 395 nm, 1 W) were fixed on the sides of an aluminum long tetragonal stand with 6 LEDs arrays in each side. This assemble was installed in a horizontal quartz tube in the center of the reactor space. The solution content could well mixed with the aid of a circulating pump which delivered the solution to a sprayer over the quartz tube. Thus, a uniform film of the aqueous solution was formed around the tube where the most photochemical degradation was expected to occur with a low mass transfer resistance. To adjust the solution temperature during each experiment, an external stream, conducted from a thermostat (0.1 °C precision), was flowed in a double path stainless steel coil, installed close the reactor bottom. The major advantage is the use of adaptable UV-LED sources and that the tetragonal installation gives a perfect 360° irradiation domain inside the reactor space. Another advantage is the formation of falling film around the quartz tube allowing oxidant-light interaction and efficient persulfate activation.

For performing each experiment, an aqueous solution with FLX initial concentration of 40 mg/L was prepared. Recently, Roshanfekr Rad et al. (2023) examined a wide concentration range of (10–200) mg/L and mostly utilized 50 mg/L initial concentrations of FLX-HCl to investigate its adsorption and photocatalytic degradation. Upon preparing drug solutions, certain amounts of potassium persulfate (within 15–200 mg/L) and ferrous sulfate heptahydrate (within 0.1–5 mg/L) were added and the pH was adjusted to a desired value by adding a low amount of either HCl or NaOH dilute solutions with the aid of a calibrated pH meter (Denver, UB-10). The prepared solution was then transferred to the photo-reactor. After turning on the LEDs, 3 mL samples were taken regularly for analyzing the reactor content while degradation was in progress.

2.3. Analytical methods

Analysis was done through absorbance measurements by means of a UV–visible spectrophotometer (Jasco, V-630, Japan). The calibration curve was first established to determine the fluoxetine concentration in the samples (Fig. 2), corresponding to the absorbance at the fluoxetine maximum wavelength ($\lambda_{max} = 226$ nm). Absorbance values of 1.535 and 0.202 were relevant to 40 and 5 mg/L FLX concentrations and consistent with the Lambert-beer law. Worth noting, there was no sensible change (less than 0.3% deviations) in the absorbance under various applied pHs for concentrations less than 40 mg/L of FLX. Then, the degradation efficiency percentage, DE (%) of fluoxetine was calculated from

$$DE\,(\%) = \frac{[\text{FLX}]_0 - [\text{FLX}]}{[\text{FLX}]_0} \times 100 \qquad (8)$$

where $[\text{FLX}]_0$ and $[\text{FLX}]$ indicate the initial fluoxetine concentration and at a specified time, respectively. Further, liquid chromatography-mass spectrometry (LC-MS) (Agilent 6410, USA)

analysis was performed to identify the transformation products while the process was in progress.

3. Results and discussion

3.1. Persulfate effect

Oxidant concentration is important in a degradation process. As indicated by Fig. 3, degradation efficiency was first increased and then remained almost constant with PS concentration. The best FLX degradation was achieved at the lowest effective PS concentration of about 100 mg/L and no sensible change was revealed with higher amounts as indicated by the inset figure. By increasing the PS concentration, formation of sulfate anion radicals and hydroxyl radicals raise; however, degradation is inhibited by the reaction of excess PS with sulfate radicals (Eq. (9), giving a lower oxidation of the target organic pollutant (Matzek and Carter, 2016).

$$S_2O_8^{2-} + SO_4^{-} \rightarrow SO_4^{2-} + S_2O_8^{-} \qquad (9)$$

3.2. pH effect

The formation of free radicals and their activity are influenced by the solution pH. Fig. 4 presents the results of FLX degradation under different pHs. Enhancing pollutant degradation from acidic to initial neutral pH is known to be due to the increase of hydroxyl ions, which causes more hydroxyl radical, $HO^{\cdot}$, generation (Liu et al., 2022). Under alkaline pHs, on the other hand, sulfate anion radical, SO_4^{-}, reacts with OH^{-} anion to produce $HO^{\cdot}$ species (Eq. (3). Although conversion of SO_4^{-} to SO_4^{2-} and producing $HO^{\cdot}$ radical with the redox potential of 2.8 V (slightly more than redox potential of SO_4^{-}, 2.5–3.1 V) is crucial, but SO_4^{2-} may act as $HO^{\cdot}$ radical scavenger at elevated concentrations (Eq. (5). Evidently, there is an optimum point for the system pH, which is the solution natural
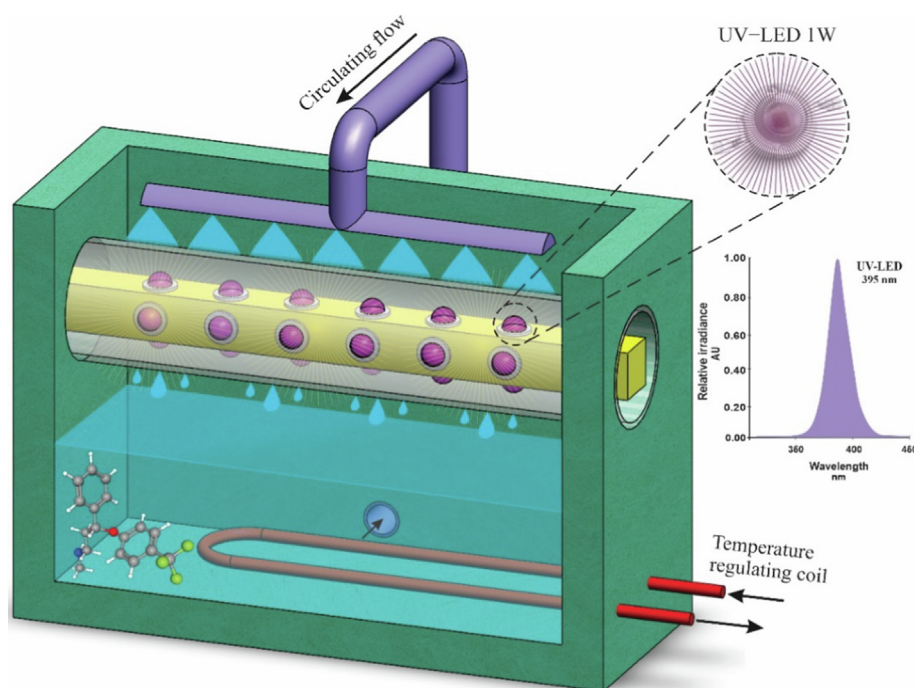

Fig. 1. The overview of the photo-reactor set-up and the scheme of a LED with the relevant light spectrum.
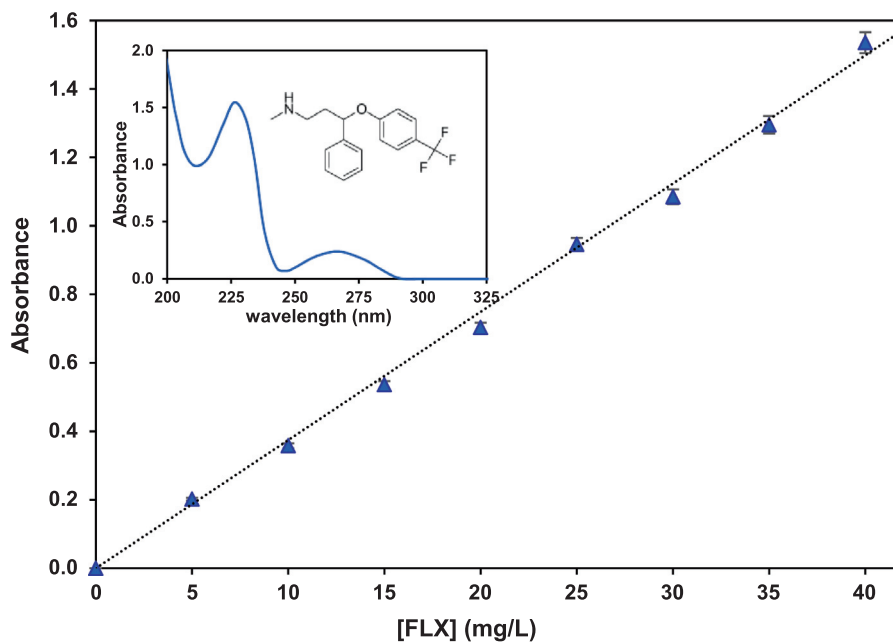
Fig. 2. Calibration curve of FLX aqueous solutions at λ_{max} = 226 nm under natural pH = 6.4. The inset represents the UV–visible spectrum of 40 mg/L of the target FLX solution. Error bars represent the standard deviation from three replicates.
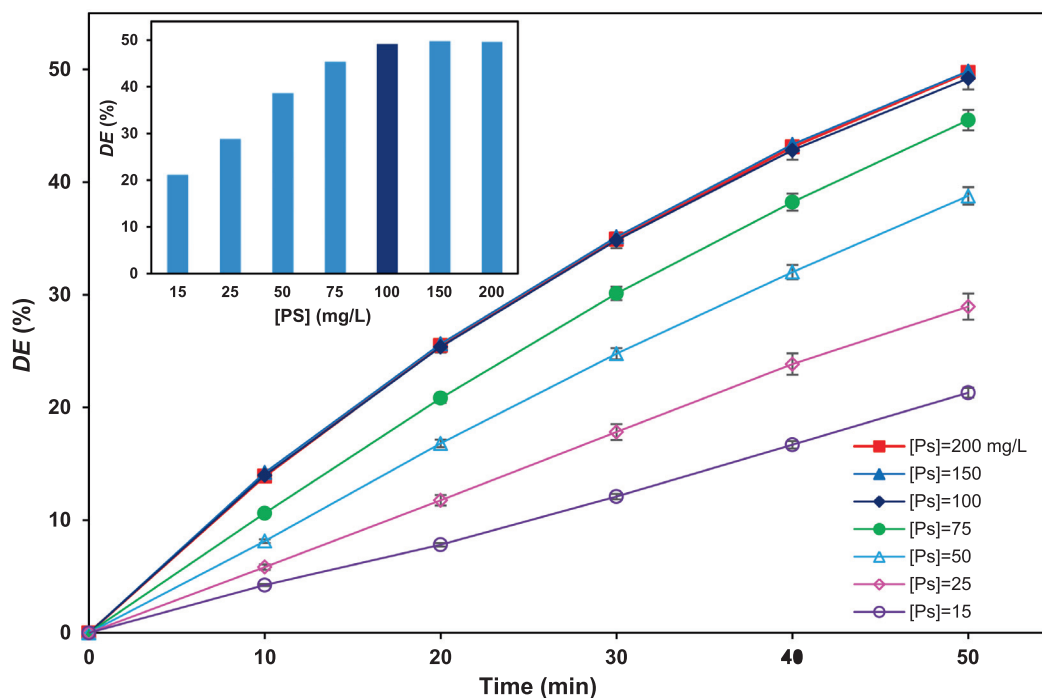

Fig. 3. Variation of degradation efficiency vs. time with different PS concentrations; [FLX]$_0$ = 40 mg/L and natural pH = 6.4. The inset figure represents the degradation efficiency versu PS concentration after 50 min. Error bars represent the standard deviation from three replicates.

pH of 6.4. Hence, pHs more than this value cause significant diminishing in degradation efficiency.

3.3. Ferrous ion effect

As presented by Eq. (6), ferrous ion can activate PS and significantly enhance the degradation efficiency. Fig. 5 shows that degra-

dation efficiency initially increases with ferrous sulfate dosage, but excessive amounts may act as radical scavenger in the way that reaction between Fe^{2+} cations and SO_4^- radical anions takes place and Fe^{2+} may convert to Fe^{3+} rapidly:

$$Fe^{2+} + SO_4^- \rightarrow Fe^{3+} + SO_4^{2-} \tag{10}$$
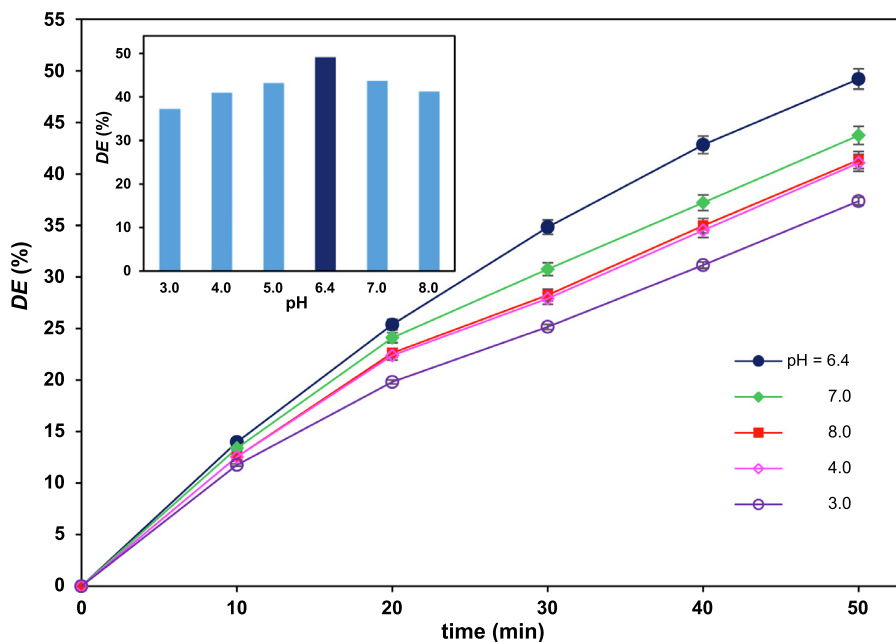
Fig. 4. Variation of degradation efficiency vs. time under different pHs; $[FLX]_0 = 40$ mg/L and $[PS] = 100$ mg/L. The inset figure represents the degradation efficiency vs. pH after 50 min. Error bars represent the standard deviation from three replicates.
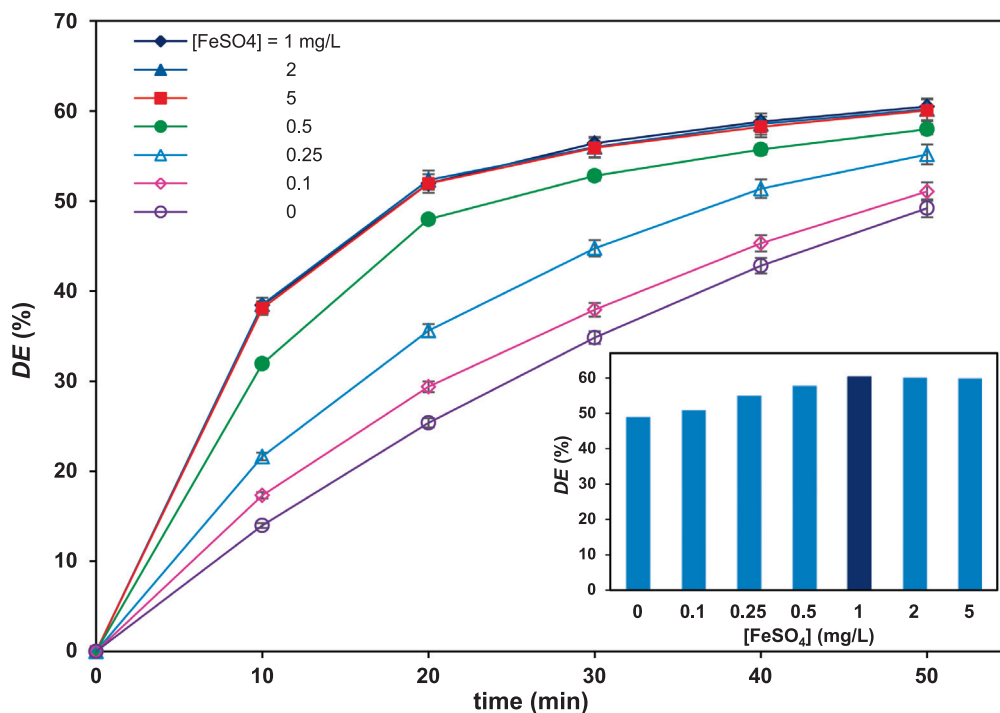

Fig. 5. Variation of degradation efficiency vs. time at different ferrous sulfate concentrations; $[FLX]_0 = 40$ mg/L, $[PS] = 100$ mg/L, and pH = 6.4. The inset figure represents the degradation efficiency vs. $FeSO_4$ concentation after 50 min.

Therefore, PS activation with Fe^{2+} ions may be limited through sulfate anion radical scavenging when excess amount of Fe^{2+} be used (Zhao et al., 2014). Thus, the optimal Fe^{2+} dosage was relevant to the very low dosage of 1 mg/L.

3.4. Temperature effect

Previous studies indicate that PS can be effectively activated upon heating, leading to more oxidation and contaminant transformation (Saien and Jafari, 2022).
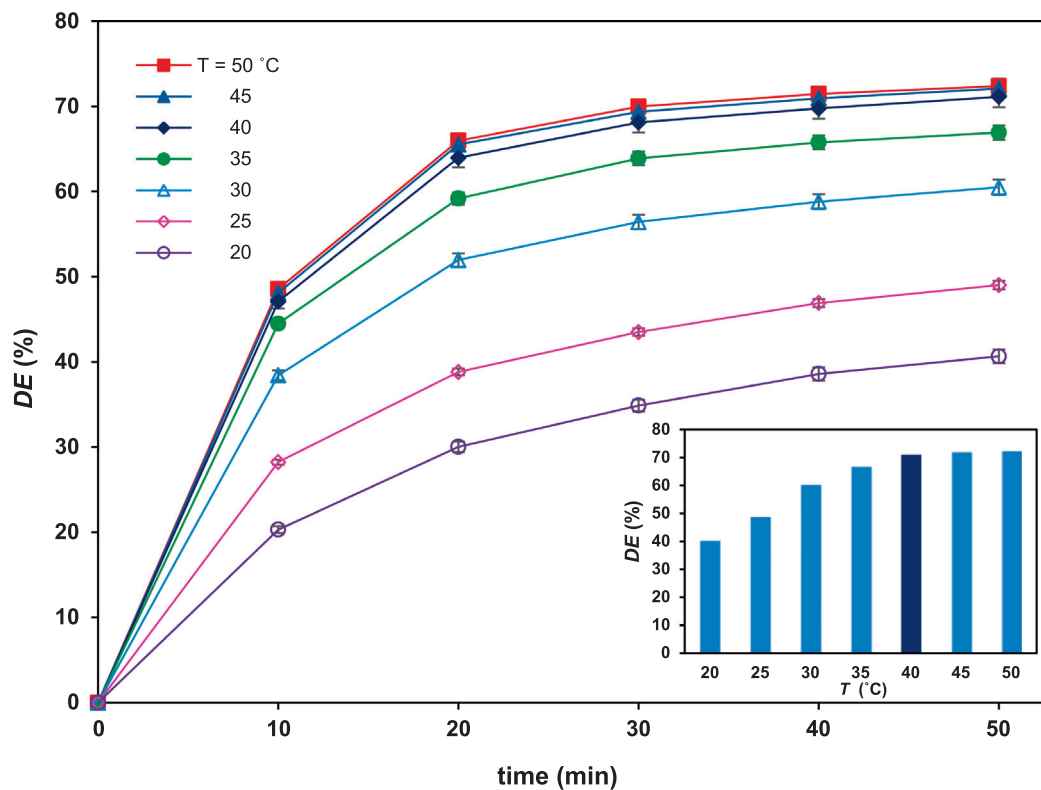
Fig. 6. Variation of degradation efficiency vs. time at different temperatures; $[FLX]_0$ = 40 mg/L, $[PS]$ = 100 mg/L, $[FeSO_4]$ = 1 mg/L, and pH = 6.4. The inset figure represents the degradation efficiency vs. temperature after 50 min.
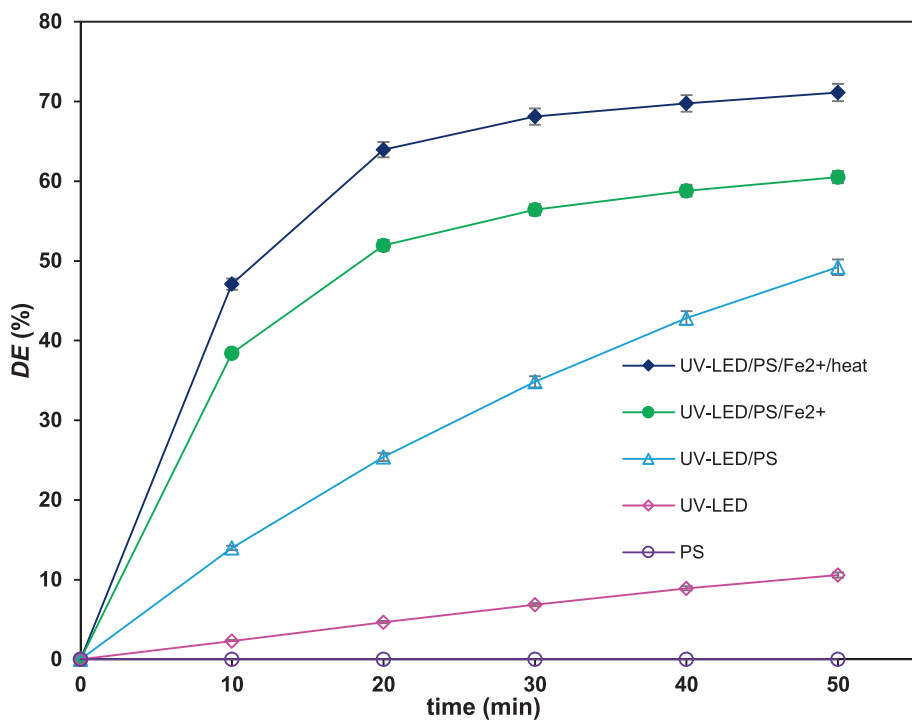
Fig. 7. Variation of degradation efficiency vs. time for different involved processes under optimum conditions; $[FLX]_0$ = 40 mg/L.
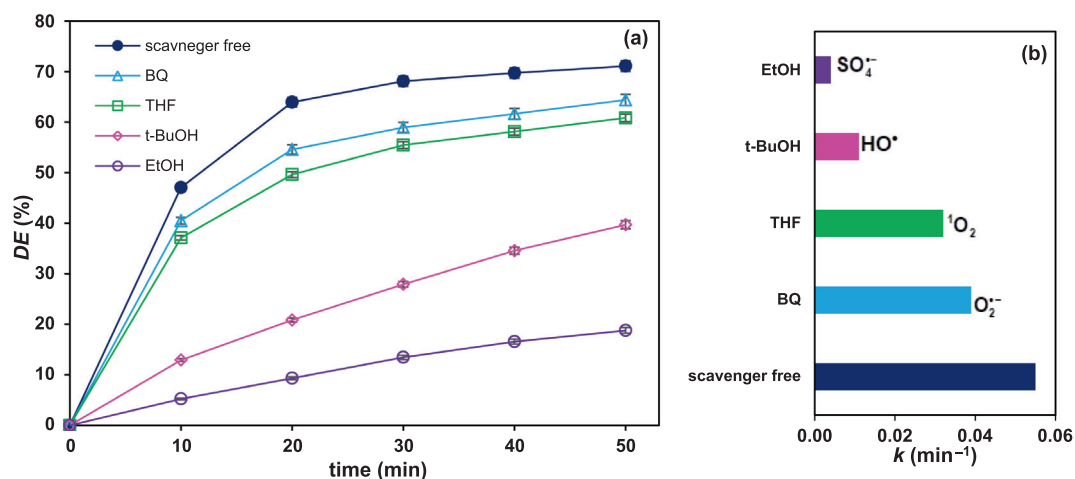
Fig. 8. Variation of FLX degradation versus time with different scavengers (4%, v/v) under optimum conditions (a), and the corresponding rate constants (b).
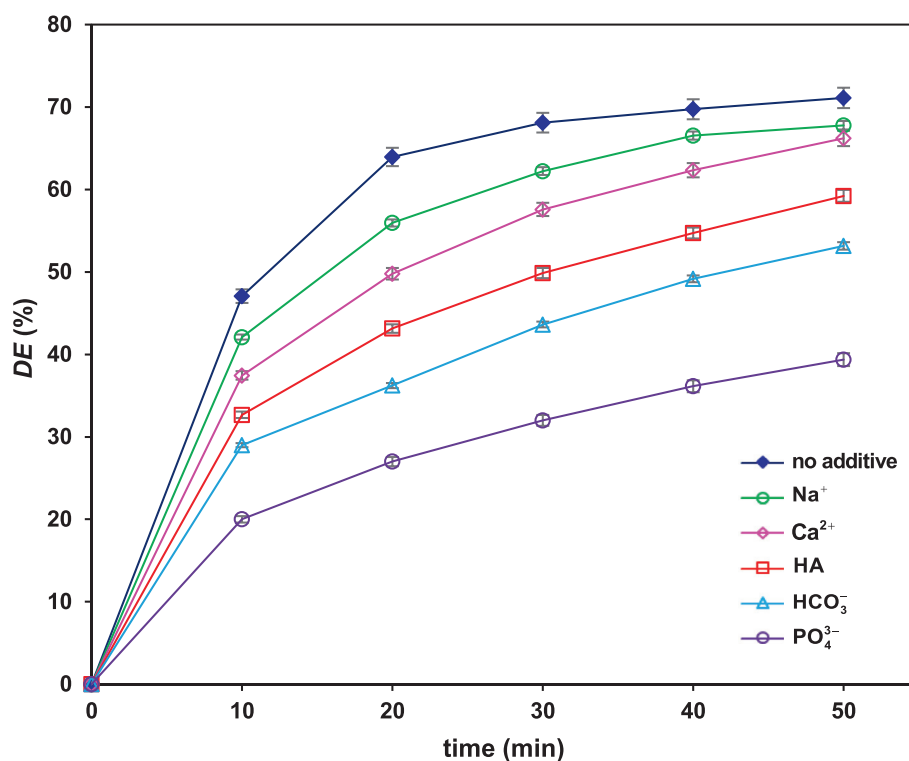
Fig. 9. Variation of degradation efficiency versus time in the presence of different ions and humic acid all with the concentration of 20 mg/L under optimum conditions.

$$S_2O_8^{2-} \overset{heat}{\rightarrow} 2SO_4^- \qquad (11)$$

The degradation of FLX under different temperatures is depicted in Fig. 6, indicating significant degradation enhancement with temperature. It is evident from the inset figure that the best performance of the degradation process is relevant to 40 °C. At higher temperatures, the energy consumption and economic criterion are not sensibly justified with respect to real industrial conditions.

3.5. Evaluating alternative operations

Aiming to evaluate the performance of alternative operations, the degradation efficiency was assessed for different processes under the found optimum conditions. As Fig. 7 illustrates, the FLX degradation efficiency was appeared in the order of: UV-LED/PS/Fe^{2+}/heat > UV-LED/PS/Fe^{2+} > UV-LED/PS > UV-LED > PS. When PS being used alone (dark, no ferrous salt), FLX does not tend to degrade and remains stable in the aqueous media since PS does not undergo activation. It was while light irradiation, ferrous ions and heat, significantly improve the PS activation and enhance the process performance to 71.1%.

3.6. Effectiveness of radicals

The effectiveness of $HO^{\cdot}$ and SO_4^- radicals was investigated by the action of scavengers. Ethanol (EtOH) and tertiary-butanol (t-
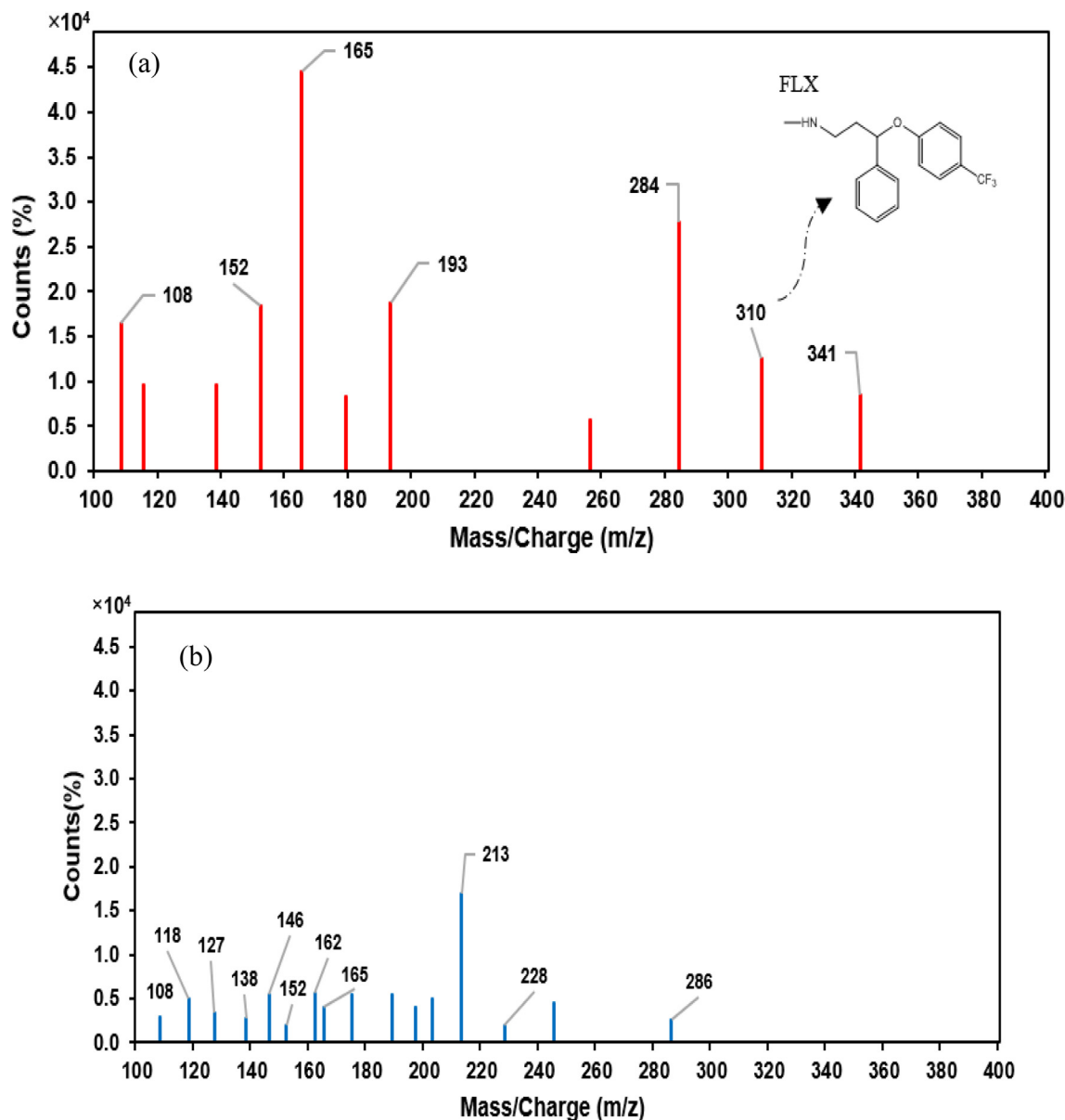
Fig. 10. LC-MS patterns of solutions before (a) and after (b) the degradation process.

BuOH) were the quenching radical scavengers exhibiting different reaction rates. Ethanol reacts rapidly with both the $HO^.$ and SO_4^- radicals; but, *tert*-butanol tends to scavenge only $HO^.$ radicals. Previous investigations indicate that the rate constant of *tert*-butanol reaction with $HO^.$ is about 1000 folds of that with SO_4^- (Lee et al., 2021; Saien and Seyyedan, 2019). As depicted in Fig. 8 (a), addition of 4% (v/v) ethanol to the solution, under optimal conditions, caused the FLX degradation efficiency to fall from 71.1 to 18.8% after 50 min; while the same dose of *tert*-butanol, caused a 31.4% decrease in degradation. Moreover, the probable presence of singlet oxygen, $^1O_2$, and superoxide anion, O_2^-, were identified using the tetrahydrofuran and 1,4-benzoquinone scavengers, respectively. Results show gradual decrease in degradation, from 71.12 to 60.8 and 64.4%, after 50 min, respectively.

Based on the above results, the contribution of reactive oxidizing species of sulfate anion radical, hydroxyl radical, singlet oxygen and superoxide anion were, respectively, 52.3, 31.4, 10.2 and 6.1%. The relevant pseudo first order rate constants are presented in Fig. 8 (b). Worth mentioning, singlet oxygen could be generated in catalytic activation of persulfate with transition metals, e.g. Cu^{3+} and Fe^{3+}. Hence, persulfate is initially hydrolyzed with Fe^{3+} and then produces the superoxide radicals (O_2^-). In the next step, the singlet oxygen ($^1O_2$) is derived from the direct oxidation of superoxide anions (Zhou et al., 2021).

3.7. Influence of water matrix

Fig. 9 depicts the effects of the presence of 20 mg/L of several water matrix compounds of HCO_3^-, PO_4^{3-}, Na^+, Ca^{2+} and
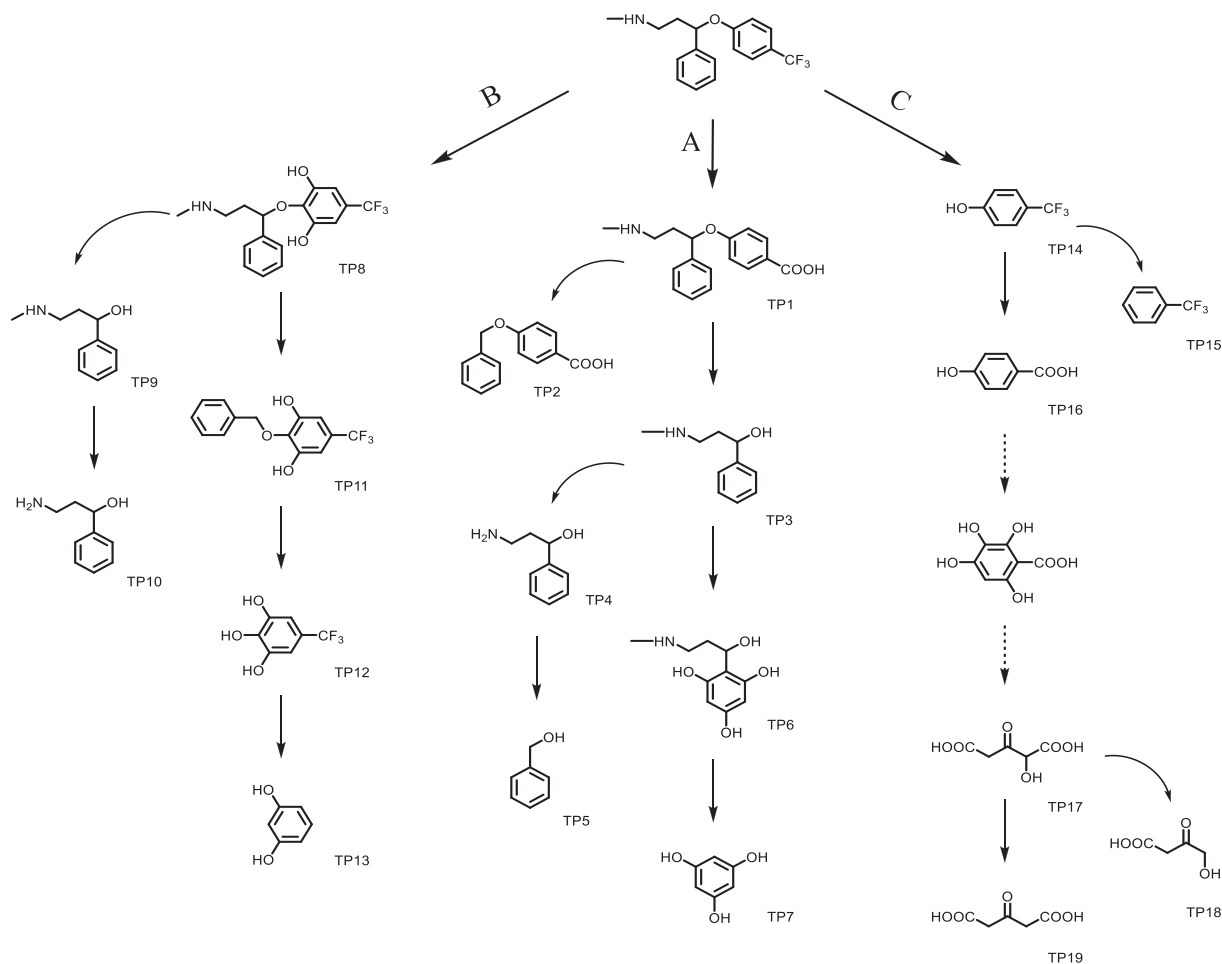
Fig. 11. Proposed degradation pathways and transformation products in the degradation process.

humic acid (HA) on the degradation of FLX in the UV-LED/PS/Fe^{2+}/heat process. The observed retarding effect of HCO_3^- on degradation efficiency can be attributed to its radical scavenging capability with sulfate radical anion which leads to generating CO_3^{-} with lower reactivity compared to $HO^{\cdot}$ and SO_4^{-} (Zhao, et al., 2016).

In the presence of PO_4^{3-} anion, the significant decline in degradation efficiency, from 71. 1 to 39.3%, can be attributed to the radical scavenging role of the anion, and that the Fe^{2+} and Fe^{3+} may form a precipitant compound with PO_4^{3-}, resulting in low availability for persulfate activation and decreasing fluoxetine degradation (Zhao, et al., 2016).

The non-significant effects of Na$^+$ and Ca^{2+} on degradation efficiency (below 7%) reveals that they neither activate persulfate (something like Fe^{2+}), nor significantly diminish the degradation efficiency. The reaction between the accompanied chloride anion with active oxidizing species can be the reason of the low decrease in degradation efficiency for this case.

Finally, presence of humic acid (HA) as a typical natural organic substrate, competing with the pollutant in oxidation process, causes significant decrease in degradation efficiency from 71.1%

to 59.2% in agreement with the investigation reported by Liu et al. (2021).

3.8. Transformation products and proposed pathways

In this study, the transformation products and reaction pathways in FLX degradation were followed via LC-MS analysis. Fig. 10 shows the patterns before and after degradation process with the profound UV-LED/PS/Fe^{2+}/heat preferred process. After degradation process, major peaks in the spectrum of before treatment sample disappeared and a number of low intensity peaks are appeared, indicating various degradation products. The proposed mechanism in the three proposed pathways of A, B and C, corresponding to the, respectively, initiate oxidation, hydroxylation and cleavage of the ether bonds of the FLX molecule, are proposed. The subsequent oxidation, hydroxylation, cleavage of bonds, decarboxylation and ring-opening phenomena occurs in either of the considered pathways are consistent with the observed peaks. Nineteen transformation products were identified as illustrated in Fig. 11 through the proposed pathways. Details of the peaks, chemical formula, mechanism of formation and their structure are listed in Table 1.

Table 1
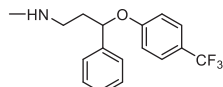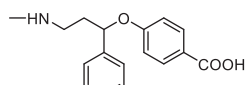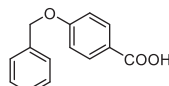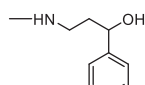The transformation products (TPs) of FLX, identified by LC-MS analysis.
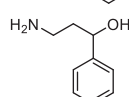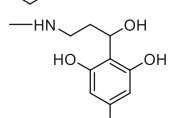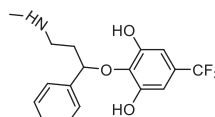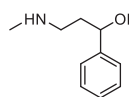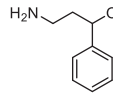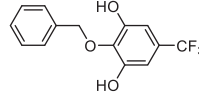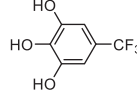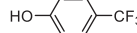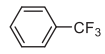
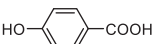| Transformation product	Observed peak (m/z)	Elemental composition	Mechanism	Proposed structure	Ref.
FLX	310	$C_{17}H_{18}F_3NO$	–		–
TP1	286	$C_{17}H_{19}NO_3$	Oxidation		(Lam et al., 2005)
TP2	228	$C_{14}H_{12}O_3$	Cleavage of C–C bond		–
TP3	165	$C_{10}H_{15}NO$	Cleavage of ether bond		(Moreira et al., 2019)
TP4	152	$C_9H_{13}NO$	Cleavage of C-N bond		(Maślanka et al., 2013)
TP5	108	C_7H_8O	Cleavage of C–C bond		–
TP6	213	$C_{10}H_{15}NO_4$	Hydroxylation		(Silva et al., 2016)
TP7	127	$C_6H_6O_3$	Cleavage of C–C bond		–
TP8	341	$C_{17}H_{18}F_3NO_3$	Hydroxylation		–
TP9	165	$C_{10}H_{15}NO$	Cleavage of ether bond		–
TP10	152	$C_9H_{13}NO$	Cleavage of C-N bond		–
TP11	284	$C_{14}H_{11}F_3O_3$	Cleavage of C–C bond		–
TP12	193	$C_7H_5F_3O_3$	Cleavage of ether bond		–
TP13	108	$C_5H_6O_5$	Cleavage of C-O bond and C–C bond		–
TP14	162	$C_7H_5F_3O$	Cleavage of ether bond		(Bai et al., 2020)
TP15	146	$C_7H_5F_3$	Cleavage of C-O bond		–

Table 1 (continued)
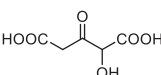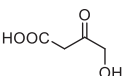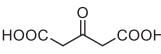
Transformation product	Observed peak (m/z)	Elemental composition	Mechanism	Proposed structure	Ref.
TP16	138	$C_7H_6O_3$	Oxidation	HO—⟨benzene⟩—COOH	(Hollman et al., 2020)
TP17	162	$C_6H_6O_6$	Ring-opening	HOOC—C(=O)—COOH, OH	(Bai et al., 2020)
TP18	118	$C_4H_6O_4$	Decarboxylation	HOOC—C(=O)—OH	–
TP19	146	$C_5H_6O_5$	Cleavage of C-O bond	HOOC—C(=O)—COOH	–

3.9. Kinetic study

The FLX degradation kinetic was studied based on the profound UV-LED/PS/Fe^{2+}/heat process under optimum conditions. The reaction order and the rate constant values were sought based on experimental data. The kinetic equation can be expressed as the variation of the degradation rate (r) versus concentration of FLX in the aqueous solution at different times (t) in the general form of:

$$r = -\frac{d[FLX]}{dt} = k[FLX]^n \qquad (12)$$

where k stands for rate constant, and n for the order. From results, the experimental data were regenerated well with a pseudo-first order kinetic and the corresponding rate constant was 0.0551 min^{-1} with the coefficient of determination (R^2) of 0.9987. Thus, an overall pseudo-first order reaction was relevant for the FLX degradation under the optimal conditions.

3.10. Energy consumption and operating cost evaluation

The level of energy consumption and the cost evaluation are essential in the study of wastewater treatment processes. Operating cost consists of major costs of electrical energy (EC), and the chemicals. The following equation has been previously proposed for electrical energy consumption in a photochemical process for one order of magnitude reduction in the substrate concentration (Bolton et al., 2001, Parsa et al., 2022):

$$E_{EC} = \frac{1000 \times P \times t}{60 \times V \times \log(C_i/C_f)} \qquad (13)$$

where P is the electrical power consumption in kW, V is the volume (in liter) of the treating solution and t is the required time to reach one order of magnitude substrate degradation. For a first order degradation, the rate constant of k (min^{-1}) can be expressed as $\ln(C_i/C_f)/t$ and thus, the above equation can be simplified as (Li et al., 2020):

$$E_{EC} = \frac{38.4 \times P}{V \times k} \qquad (14)$$

In view of that, the electrical energy consumption of the as described UV-LED/PS/Fe^{2+}/heat process was calculated as 16.7 kWh/m^3. Considering the electrical energy cost in the industrial sector of United States as 0.0934 \$/kWh in September 2022 (EIA, 2022), the energy cost would be 1.56 \$/m^3. By adding the cost

of chemicals ($K_2S_2O_8$: 1.5 \$/kg and $FeSO_4.7H_2O$: 0.2 \$/kg, alibaba.com), the total operating cost was roughly evaluated as low as 1.71 \$/m^3. Therefore, the proposed process brings about a high efficiency and low operating cost mainly due to the high performance of the employed photo-reactor and benefits of utilizing LED light sources as well as low price reagents. In a recent study by Moreira et al., (2019), four UV lamps have been used (each 15 W) for degradation of 10 mL solutions of fluoxetine. Based on Eq. (14), the relevant energy consumption would be 36.7 kWh/m^3, much higher than the corresponding value in this study.

4. Conclusions

Degradation of fluoxetine drug in aqueous media was attainable using a mild homogeneous process with persulfate oxidant while irradiated with ultraviolet light-emitting diodes. From discussions, the following more important conclusions are drawn:

- Persulfate activation was feasible by using UV-LEDs with proper circular irradiating the provided falling film, leading to effective degradation of the resistive drug.
- Presence of ferrous ion and heating the media could significantly improve the process performance due to efficient interactions with persulfate.
- Based on the obtained degradation efficiency, the used processes were efficient in the order of: UV-LED/PS/Fe^{2+}/heat > UV-LED/PS/Fe^{2+} > UV-LED/PS > UV-LED > PS.
- The scavenging test indicated that sulfate anion and hydroxyl radicals had the major contribution in the degradation process, whereas singlet oxygen and superoxide anion contributed minor.
- Identifying the transformation products elucidated the reaction pathways and degradation steps toward mineralization.
- Thanks to the LED utilization and the low price reagents, the proposed process requires low electrical energy consumption of 16.7 kWh/m^3 and operating cost of 1.71 \$/m^3.

Noteworthy, the rather long time activation of persulfate and remaining sulfate species in the media are remarkable limitations for the process. The future works to accomplish this investigation could involve examining real pharmaceutical wastewaters, gradual addition of the reagents, using alternative oxidants like peroxymonosulfate, as well as employing ultrasound devices.

Authors Contributions

The authors contributed to the study conception and design. Set-up design, material preparation, data collection and analysis were performed by J. Saien and H. Karbalaei Abbas. The supervision and evaluating the consistency of data as well as review and organizing the manuscript were performed by J. Saien and F. Jafari. The authors read and approved the final manuscript.

Declaration of Competing Interest

The authors declare that they have no known competing financial interests or personal relationships that could have appeared to influence the work reported in this paper.

Acknowledgment

References

Alibaba Wholesale Trade Company, http://www.alibaba.com.

Bai, R., Yan, W., Xiao, Y., Wang, S., Tian, X., Li, J., Xiao, X., Lu, X., Zhao, F., 2020. Acceleration of peroxymonosulfate decomposition by a magnetic MoS_2/$CuFe_2O_4$ heterogeneous catalyst for rapid degradation of fluoxetine. J. Chem. Eng. 397, 125501.

Bolton, J., Bircher, K.G., Tumas, W., Tolman, C.A., 2001. Figures-of-merit for the technical development and application of advanced oxidation technologies for both electric-and solar-driven systems. Pure Appl. Chem. 73, 627–637.

Cai, A., Deng, J., Zhu, T., Ye, C., Li, J., Zhou, S., Li, Q., Li, X., 2021. Enhanced oxidation of carbamazepine by UV-LED/persulfate and UV-LED/H_2O_2 processes in the presence of trace copper ions. J. Chem. Eng. 404, 127119.

Chakma, S., Praneeth, S., Moholkar, V.S., 2017. Mechanistic investigations in sono-hybrid (ultrasound/Fe^{2+}/UVC) techniques of persulfate activation for degradation of Azorubine. Ultrason. Sonochem. 38, 652–663.

Chen, J., Loeb, S., Kim, J.H., 2017. LED revolution, fundamentals and prospects for UV disinfection applications. Environ. Sci. Water Res. Technol. 3, 188–202.

Duan, X., He, X., Wang, D., Mezyk, S.P., Otto, S.C., Marfil-Vega, R., Mills, M.A., Dionysiou, D.D., 2017. Decomposition of iodinated pharmaceuticals by UV-254 nm-assisted advanced oxidation processes. J. Hazard. Mater. 323, 489–499.

Eskandarian, M.R., Ganjkhanloo, M., Rasoulifard, M.H., Hosseini, S.A., 2021. Energy-efficient removal of acid red 14 by UV-LED/persulfate advanced oxidation process, pulsed irradiation, duty cycle, reaction kinetics, and energy consumption. J. Taiwan Inst. Chem. Eng. 127, 129–139.

Hoang, N.T., Nguyen, V.T., Minh, T., Manh, T.D., Le, P., Van Tac, D., Mwazighe, F.M., 2022. Degradation of dyes by UV/Persulfate and comparison with other UV-based advanced oxidation processes, Kinetics and role of radicals. Chemosphere 298, 134197.

Hollman, J., Dominic, J.A., Achari, G., 2020. Degradation of pharmaceutical mixtures in aqueous solutions using UV/peracetic acid process, Kinetics, degradation pathways and comparison with UV/H_2O_2. Chemosphere 248, 125911.

Kanakaraju, D., Glass, B.D., Oelgemöller, M., 2018. Advanced oxidation process-mediated removal of pharmaceuticals from water, a review. J. Environ. Manage. 219, 189–207.

Kwon, J.W., Armbrust, K.L., 2009. Laboratory persistence and fate of fluoxetine in aquatic environments. Environ. Toxic. Chem. 25, 2561–2568.

Lam, M.W., Young, C.J., Mabury, S.A., 2005. Aqueous photochemical reaction kinetics and transformations of fluoxetine. Environ. Sci. Tech. 39, 513–522.

Lau, T.K., Chu, W., Graham, N.J., 2007. The aqueous degradation of butylated hydroxyanisole by UV/$S_2O_8^{2-}$, study of reaction mechanisms via dimerization and mineralization. Environ. Sci. Tech. 41, 613–619.

Lee, Y.M., Lee, G., Zoh, K.D., 2021. Benzophenone-3 degradation via UV/H_2O_2 and UV/persulfate reactions. J. Hazard. Mater. 403, 123591.

Li, B., Ma, X., Deng, J., Li, Q., Chen, W., Li, G., Chen, G., Wang, J., 2020. Comparison of acetaminophen degradation in UV-LED-based advance oxidation processes, reaction kinetics, radicals contribution, degradation pathways and acute toxicity assessment. Sci. Total Environ. 723, 137993.

Liu, Y., Ji, X., Yang, J., Tang, W., Zhu, Y., Wang, Y., Zhang, Y., Zhang, Y., Duan, J., Li, W., 2022. Degradation of the typical herbicide atrazine by UV/persulfate, kinetics and mechanisms. Environ. Sci. Pollut. Res. 29, 43928–43941.

Liu, S., Zhang, Z., Huang, F., Liu, Y., Feng, L., Jiang, J., Zhang, L., Qi, F., Liu, C., 2021. Carbonized polyaniline activated peroxymonosulfate (PMS) for phenol degradation: role of PMS adsorption and singlet oxygen generation. Appl Catal B 286, 119921.

Marchetti, M., Azevedo, E., 2020. Degradation of NSAIDs by optimized photo-Fenton process using UV-LEDs at near-neutral pH. J. Water Process Eng. 35, 101171.

Martin, J., Saaristo, M., Bertram, M., Lewis, P., Coggan, T., Clarke, B., Wong, B., 2017. The psychoactive pollutant fluoxetine compromises antipredator behaviour in fish. Environ. Pollut. 222, 592–599.

Maślanka, A., Hubicka, U., Krzek, J., Walczak, M., Izworski, G., 2013. Determination of fluoxetine in the presence of photodegradation products appearing during UVA irradiation in a solid phase by chromatographic-densitometric method, kinetics and identification of photoproducts. Acta Chromatogr. 25, 465–481.

Matafonova, G., Batoev, V., 2018. Recent advances in application of UV light-emitting diodes for degrading organic pollutants in water through advanced oxidation processes. A review. Water Res. 132, 177–189.

Matzek, L.W., Carter, K.E., 2016. Activated persulfate for organic chemical degradation, a review. Chemosphere 151, 178–188.

Méndez-Arriag, F., Otsu, T., Oyama, T., Gimenez, J., Esplugas, S., Hidaka, H., Serpone, N., 2011. Photooxidation of the antidepressant drug Fluoxetine (Prozac®) in aqueous media by hybrid catalytic/ozonation processes. Water Res. 45, 2782–2794.

Moreira, A.J., Borges, A.C., Sousa, B.B., Mendonça, V.R., Freschi, C.D., Freschi, G.P., 2019. Photodegradation of fluoxetine applying different photolytic reactors, evaluation of the process efficiency and mechanism. J. Braz. Chem. Soc. 30, 1010–1024.

Muramoto, Y., Kimura, M., Nouda, S., 2014. Development and future of ultraviolet light-emitting diodes, UV-LED will replace the UV lamp. Semicond. Sci. Technol. 29, 084004.

Parsa, J.B., Alamdar, M., Jafari, F., 2022. Integrated ozone-sono-Fenton for the enhanced degradation of acid orange 7, process optimization and kinetic evaluation. Environ. Sci. Pollut. Res. 29, 78444–78456.

Pourehie, O., Saien, J., 2020. Homogeneous solar Fenton and alternative processes in a pilot-scale rotatable reactor for the treatment of petroleum refinery wastewater. Process Saf. Environ. Prot. 135, 236–243.

Rasheed, T., Ahmad, N., Ali, J., Hassan, A.A., Sher, F., Rizwan, K., Iqbal, H.M., Bilal, M., 2021. Nano and micro architected cues as smart materials to mitigate recalcitrant pharmaceutical pollutants from wastewater. Chemosphere 274, 129785.

Redshaw, C.H., Cooke, M.P., Talbot, H.M., McGrath, S., Rowland, S.J., 2008. Low biodegradability of fluoxetine HCl, diazepam and their human metabolites in sewage sludge-amended soil. J. Soil. Sedim. 8, 217–230.

Roshanfekr Rad, L., Anbia, M., Vatanpour, V., 2023. Adsorption and photocatalytic degradation of fluoxetine using TiO_2-supported-clinoptilolite, NaX and MIL-101 (Fe) metal organic framework. J. Inorg. Organomet. Polym Mater., 2154–2171

Saien, J., Bazkiaei, F.V., 2018. Homogeneous UV/periodate process in treatment of p-nitrophenol aqueous solutions under mild operating conditions. Environ. Technol. 39, 1823–1832.

Saien, J., Jafari, F., 2022. Methods of persulfate activation for the degradation of pollutants, fundamentals and influencing parameters, Chapter 1. In: Zhu, M., Zhao, C., Bian, Z. (Eds.), Persulfate-Based Oxidation Processes in Environmental Remediation. Pub. RSC.

Saien, J., Seyyedan, S., 2019. High performance homogeneous photo-activated persulfate for nicotinic acid removal, intensified with copper ions and ultrasonic waves. Process Saf. Environ. Prot. 131, 300–306.

Sicras-Mainar, A., Navarro-Artieda, R., 2016. Use of antidepressants in the treatment of major depressive disorder in primary care during a period of economic crisis. Neuropsychiatr. Dis. Treat. 12, 29–40.

Silva, V.O., dos Santos Batista, A.P., Teixeira, S.C., Borrely, S.I., 2016. Degradation and acute toxicity removal of the antidepressant fluoxetine (Prozac®) in aqueous systems by electron beam irradiation. Environ. Sci. Pollut. Res. 23, 11927–11936.

Silva, L., Lino, C., Meisel, L., Pena, A., 2012. Selective serotonin re-uptake inhibitors (SSRIs) in the aquatic environment, an ecopharmacovigilance approach. Sci. Total Environ. 437, 185–195.

Sun, Q., Fan, Y., Yang, J., Lu, Z., Xu, Z., Lai, X., Zheng, Y., Cai, K., Wang, F., 2022. Role of trace TEMPO as electron shuttle in enhancing chloroquine phosphate elimination in UV-LED-driven persulfate activation process. J. Environ. Chem. Eng. 10, 108641.

Taoufik, N., Boumya, W., Achak, M., Sillanpää, M., Barka, N., 2021. Comparative overview of advanced oxidation processes and biological approaches for the removal pharmaceuticals. J. Environ. Manage. 288, 112404.

Tiwari, B., Sellamuthu, B., Ouarda, Y., Drogui, P., Tyagi, R.D., Buelna, G., 2017. Review on fate and mechanism of removal of pharmaceutical pollutants from wastewater using biological approach. Bioresour. Technol. 224, 1–12.

US. Energy Information Administration (EIA), 2022 form EIA-861M (formerly EIA-826), monthly Electric Power Industry Report.

Zhao, L., Hou, H., Fujii, A., Hosomi, M., Li, F., 2014. Degradation of 1, 4-dioxane in water with heat-and Fe^{2+}-activated persulfate oxidation. Environ. Sci. Pollut. Res. 21, 7457–7465.

Zhao, Y., Zhao, Y., Li, Q., Zhou, R., Chen, X., 2016. Effect of common inorganic ions on aniline degradation in groundwater by activated persulfate with ferrous iron. Water Sci. Technol. 16, 667–674.

Zhou, X., Jawad, A., Luo, M., Luo, C., Zhang, T., Wang, H., Wang, J., Wang, S., Chen, Z., Chen, Z., 2021. Regulating activation pathway of Cu/persulfate through the incorporation of unreducible metal oxides: Pivotal role of surface oxygen vacancies. Appl. Catal. B: Environ. 286, 119914.